Review of Derivatives Research, 6, 179–202, 2003

The Dynamics of Implied Volatilities: A Common Principal Components Approach

MATTHIAS R. FENGLER * and WOLFGANG K. HÄRDLE e-mail: fengler@wiwi.hu-berlin.de
CASE – Center for Applied Statistics and Economics, Department of Business Administration and Economics, Humboldt-Universität zu Berlin, Spandauer Straße 1, 10178 Berlin, Germany

CHRISTOPHE VILLA
CREST-LSM and CREREG-University of Rennes 1, Ecole Nationale de la Statistique et de l'Analyse de l'Information (ENSAI), Rennes Métropole – Campus de Ker Lann, Rue Blaise Pascal, BP 37203, 35172 BRUZ Cedex, France

Abstract. It is common practice to identify the number and sources of shocks that move, e.g., ATM implied volatilities by principal components analysis. This approach, however, is likely to result in a loss of information, since the *surface structure* of implied volatilities is neglected. In this paper we analyze the implied volatility surface along maturity slices with a *common* principal components analysis (CPC), known from morphometrics. In CPC analysis, the space spanned by the eigenvectors is identical across groups, whereas variances associated with the common principal components vary. Our analysis shows that implied volatility surface dynamics can be traced back to a common eigenstructure in maturity slices. This empirical result is used to set up a factor model for implied volatility surface dynamics.

Keywords: common principal component analysis, principal component analysis, factor model, implied volatility surface, smile.

JEL classification: C13, C49, G13

Understanding volatility of financial assets has become a first rank issue in modern financial theory and practice: whether in risk management, portfolio hedging, or option pricing, a precise notion of the market's assessment and expectation of volatility is inevitable. Much research has been spent on *realized historic volatilities* ((Roll, 1977), and references therein). However, since it seems unsettling to draw conclusions from past to expected behavior of volatility, the focus shifted to *implied volatilities* (Dumas, Fleming, and Whaley, 1998). Implied volatilities (IV) $\hat{\sigma}$ are derived from the Black and Scholes (BS) formula given observed option prices. Inferring volatility directly from observed option prices is more natural as the option value is decisively determined by the market's assessment of current and future volatility. Hence IV may be interpreted as the market's expectation of average volatility over the remaining lifetime of the option.

The volatilities implied by observed market prices exhibit a pattern that is different from that actually assumed in the BS framework (Black and Scholes, 1973): instead of being constant across strikes K and time to maturity τ, IV appears to be nonflat. This depen-

* Corresponding author.

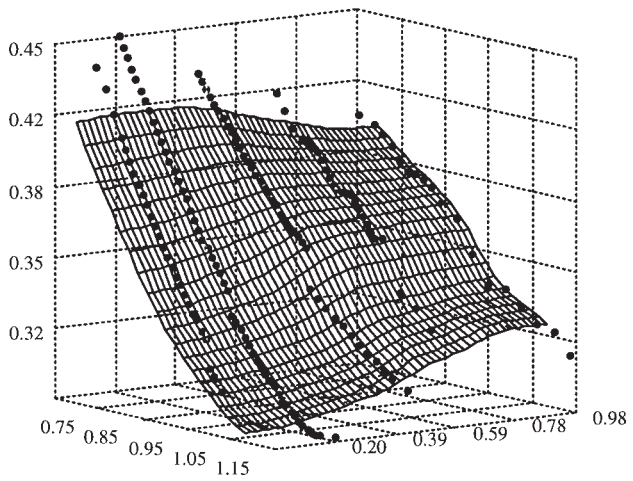

Figure 1. IVS from options on the German DAX index from January 4, 1999. The surface is obtained via the Nadaraya–Watson kernel estimator, compare Appendix A for details. Original observations displayed as black bullets. Left axis denotes moneyness defined as $K/(S_t e^{r\tau})$, where K is the strike and S_t the asset price (DAX value) in t, r the interest rate and $\tau = T - t$ time to maturity. Right axis time to maturity τ measured in years.

dence, captured by the function $\hat{\sigma}_t : (K, \tau) \to \hat{\sigma}_t(K, \tau)$, is given by the implied volatility surface (IVS). A typical picture is presented in Figure 1 showing a pronounced curvature across strikes (here, in the scale of moneyness) on January 4, 1999. For a given maturity τ, this function has been named 'smile' or, if it is skewed, 'smirk'.

A considerable amount of literature aims at reconciling this empirical finding with financial theory. This can be achieved by including an additional degree of freedom into option pricing models. Well-known examples are stochastic volatility models (Hull and White, 1987; Stein and Stein, 1991; Heston and Nandi, 2000), models with jump diffusions (Merton, 1973; Bates, 1996), or models building on general Lévy processes, such as the generalized hyperbolic process (Eberlein and Prause, 2002). However, these models generate smile and term structure phenomena that only partially capture the spectrum of functional patterns of the IVS and the complexity of its dynamics (Tompkins, 2001).

Unlike Hull and White (1987) and others, the approach taken in this paper is not to explain deformations or deviations of IV from the BS model, but to regard IV as yet another financial variable interesting by itself. At first sight, this notion seems to be unsatisfactory from a theoretical standpoint, however, it is not without merit: first, IV plays an important rôle for practitioners, since it serves as a convenient one-to-one mapping from the spaces

of option and strike prices, interest rates, and maturities to the (positive) real line. Second, with growing liquidity of organized option markets, traders are interested in investing in 'volatility' itself, i.e., in setting up portfolios that have a vega sensitivity, only. Standardized volatility products such as the VDAX (Deutsche Börse AG) and the VIX (CBOE) reflect this demand. Third, from a theoretical point of view, attention focussed recently on IVs with the emergence of the *market models of volatility* (Ledoit and Santa-Clara, 1998; Schönbucher, 1999). Market models of volatility use the existence of a sufficient number of traded plain vanilla options to price exotic and illiquid derivatives consistently with the observed IVS. In this context, Derman (1999) developed 'sticky' rules, which formulate hypotheses on the relationship of the IV smile and strike prices depending on the market regime prevailing in the current market.

Yet, practically, to set up a model that truly reflects the dynamics of IVs—be it for trading, pricing or risk management—one has to identify the number and shapes of the shocks that move the IVS across time. Borrowing from the literature of the term structure of interest rates (Rebonato, 1998), the most common technique employed is principal component analysis (PCA). When applied to the term structure of IVs of at-the-money (ATM) options (Avellaneda and Zhu, 1997; Fengler, Härdle, and Schmidt, 2002) or to a smile at a given maturity (Alexander, 2001), this approach carries directly over from the interest rate literature. However, the important difference between interest rate analysis and IV analysis is the surface structure. Derman and Kamal (1997) analyze changes in IVs by stacking the surface into a vector. Thus, surface dynamics are given by a multivariate time series and standard PCA may be applied. A grouping approach is taken by Skiadopoulos, Hodges, and Clewlow (1999) who form three 'maturity buckets' in the surface, average IVs of options whose maturities fall into them and apply PCA to each bucket covariance matrix separately. Besides neglecting the surface structure, these approaches may result in a hybrid set of principal components disturbed by both within and between group variation (Basilevsky, 1994, p. 313). Most importantly, both approaches cannot distinguish between *common* and *specific* factors that drive the IVS, a task which is at the heart of our study.

We depart from the research mentioned before in three ways: first, we estimate nonparametrically the IVS day by day with a kernel smoothing procedure. In smoothing the IVS, we recover the time series of IVs $\{\hat{\sigma}_t(\kappa, \tau)\}_{t=1}^{T}$ on a given grid of moneyness κ and maturity τ. Second, we apply a dimension reduction technique of multivariate analysis to the IVS: *common* principal component analysis. This method exploits the natural group structure in the data. Third, the presented framework allows for testing more flexible and more restrictive specifications of the model against each other.

The analysis is motivated from two salient features that characterize IVS dynamics: first, the instantaneous profile of the IVS is subject to changes, while most shocks tend to move it into the same direction. Second, the size of the shocks decreases with the option's maturity. This leads to high spatial correlation between contemporaneous surface values, while at the same time 'volatility' of IV is highest for short maturity contracts. The insight from these observations is that IVs of different maturity groups may obey a *common* eigenstructure. The *common principal components* (CPC) model exactly features this structure, Flury (1988). Mathematically, the CPC model assumes that the space spanned by the eigenvectors of the covariance matrices is identical across different groups, whereas

variances associated with the components may vary. Thus, IVS dynamics can be generated by a small number of factors from a low-dimensional space spanned by the eigenvectors of a common transformation matrix. The advantage of the CPC framework is that it is mathematically appealing, and empirically parsimonious.

Our results show that the CPC model is appropriate for analyzing the IVS, especially for short maturities. A shift, slope, and twist interpretation of IVs is revealed (Cont and da Fonseca, 2002; Fengler, Härdle, and Schmidt, 2002; Fengler, Härdle, and Mammen, 2003). Moreover, CPC models offer a convenient framework for factor models which can be exploited for Monte Carlo simulations of IVS scenarios. Thus, these models may be used for risk analysis or as partial models in more complex pricing algorithms.

In the following section, we give a graphical motivation underpinning the hypothesis of a CPC model. Section 2 describes the CPC and related models. In Section 3 the empirical results are presented and discussed. A factor model is devised based on the results. Section 5 concludes. Appendices A and B contain details on the maximum likelihood estimator and the smoothing procedure.

1. Common Principal Components

PCA, as introduced into statistics by Pearson (1901) and Hotelling (1933) is a dimension reduction technique for one group. In many applications, however, the data fall into groups in which the same variables are measured. For example, in a zoological application one measures the same characteristics across different species, or in an economic case study one observes the same variables across different countries or markets. In an analysis of the IVs, at each observation date only a limited number of maturities are traded, whereas in the strike dimension a large number of contracts exist, which is visible from the thick points in Figure 1. In all situations, it can be assumed that the overall structure observed between groups is governed by one or more common unobservable factors.

Denote $\{\hat{\sigma}_t(\kappa, \tau)\}_{t=1}^T$ the time series of IVs at time t as a function of moneyness κ and maturity τ measured in months. We define moneyness as $\kappa = K/F_t$, where K is the option's strike price, and $F_t = S_t e^{r\tau}$ the future price (Hull, 2002). As IVs are recovered on a constant grid of moneyness κ_j and moneyness τ_i (see Appendix), the time series of volatility returns, i.e., log-differences of IVs, $\{\Delta \ln \hat{\sigma}_t(\kappa_j, \tau_i)\}_{t=2}^T$, are defined. In Figure 2, we show a scatter plot of $\{\Delta \ln \hat{\sigma}_t(0.90, 1)\}_{t=2}^T$ against $\{\Delta \ln \hat{\sigma}_t(1.10, 1)\}_{t=2}^T$ in the left panel and in the right panel a scatter plot of $\{\Delta \ln \hat{\sigma}_t(0.90, 3)\}_{t=2}^T$ against $\{\Delta \ln \hat{\sigma}_t(1.10, 3)\}_{t=2}^T$, i.e., for two different maturity groups, one and three months, respectively, we plot the IV returns of two different moneyness against each other. Additionally we display the principal axes and the ellipses of constant standard distance, i.e., the Mahalanobis distance from the respective mean vector (Mardia, Kent, and Bibby, 1992):

$$\left\{(\boldsymbol{x}_i - \overline{\boldsymbol{x}}_i)^\top \boldsymbol{S}_i^{-1}(\boldsymbol{x}_i - \overline{\boldsymbol{x}}_i)\right\}^{1/2} = 2, \quad i = 1, 2, \tag{1}$$

where $\boldsymbol{x}_i \stackrel{\text{def}}{=} \Delta \ln \hat{\sigma}_t(\cdot, \tau_i)$, $\tau = 1, 3$ which corresponds $i = 1, 2$. $\boldsymbol{S}_i$ is the sample

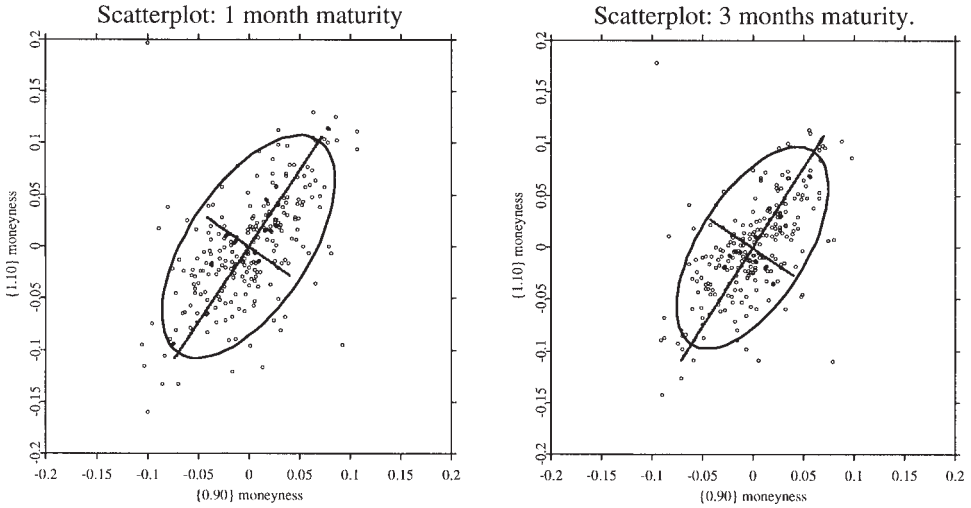

Figure 2. Scatterplots of implied volatility returns of moneyness $\kappa = 0.90$ against $\kappa = 1.10$ for groups of 1 month and 3 months time to maturity. Implied volatility returns computed as log-differences from the IVS recovered on a fixed grid; moneyness is defined as $K/(S_t e^{r\tau})$, where K is the strike and S_t the asset price (DAX value) in t, r the interest rate and $\tau = T - t$ time to maturity. The ellipse denotes the Mahalanobis distance defined in (1), which is the 95% confidence region for a bivariate normal distribution. Principle axes of the ellipses are the eigenvectors obtained by separate PCA for each maturity group, compare Figure 3.

Table 1. PCA in the Two Group Implied Volatility Case

Maturity Group	**1 Month**	**3 Months**
Sample covariance	$\boldsymbol{S}_1 = \begin{pmatrix} 0.182 & 0.137 \\ 0.137 & 0.290 \end{pmatrix}$	$\boldsymbol{S}_2 = \begin{pmatrix} 0.141 & 0.109 \\ 0.109 & 0.238 \end{pmatrix}$
Mean	$\overline{\boldsymbol{x}}_1 = \begin{pmatrix} -0.052 & -0.063 \end{pmatrix}^\top$	$\overline{\boldsymbol{x}}_2 = \begin{pmatrix} -0.054 & -0.078 \end{pmatrix}^\top$
Matrix of eigenvectors	$\hat{\boldsymbol{\Gamma}}_1 = \begin{pmatrix} 0.563 & 0.827 \\ 0.827 & -0.563 \end{pmatrix}$	$\hat{\boldsymbol{\Gamma}}_2 = \begin{pmatrix} 0.546 & 0.837 \\ 0.837 & -0.546 \end{pmatrix}$
Characteristic roots	$\hat{\lambda}_1 = \begin{pmatrix} 0.383 & 0.089 \end{pmatrix}^\top$	$\hat{\lambda}_2 = \begin{pmatrix} 0.309 & 0.070 \end{pmatrix}^\top$

Notes: The table presents eigenvectors in the matrix $\hat{\boldsymbol{\Gamma}}_i$ and eigenvalues $\hat{\lambda}_{ij}$ from a PCA applied separately to the groups of 1 and 3 months time to maturity implied volatility data: for each group $i = 1, 2$, sample covariance matrices $\boldsymbol{S}_i$ are computed from a two-dimensional time series of implied volatility returns calculated as log-differences. Each series belongs to a different moneyness in the IVS, 0.90 and 1.10, respectively. $\boldsymbol{S}_i$, $\hat{\lambda}_{ij}$, and $\overline{\boldsymbol{x}}_i$ are presented times 10^2. German DAX index option data.

covariance matrix and $\overline{\boldsymbol{x}}_i$ the mean vector in group i. The ellipse is the 95% confidence region for a bivariate normal distribution.

The principal axes or the eigenvectors $\boldsymbol{\Gamma}_i = (\boldsymbol{\gamma}_{i1}, \boldsymbol{\gamma}_{i2})$, are almost parallel (Figure 2 and Table 1). Variability, however, both reflected in the size of the eigenvalues λ_{ij} and in the size of the ellipses, is different between the two maturity groups. We recover the empirical fact that IV returns of short maturities are more volatile and hence more spread out in space than the ones of long maturities. Given these observations, it seems natural to propose a

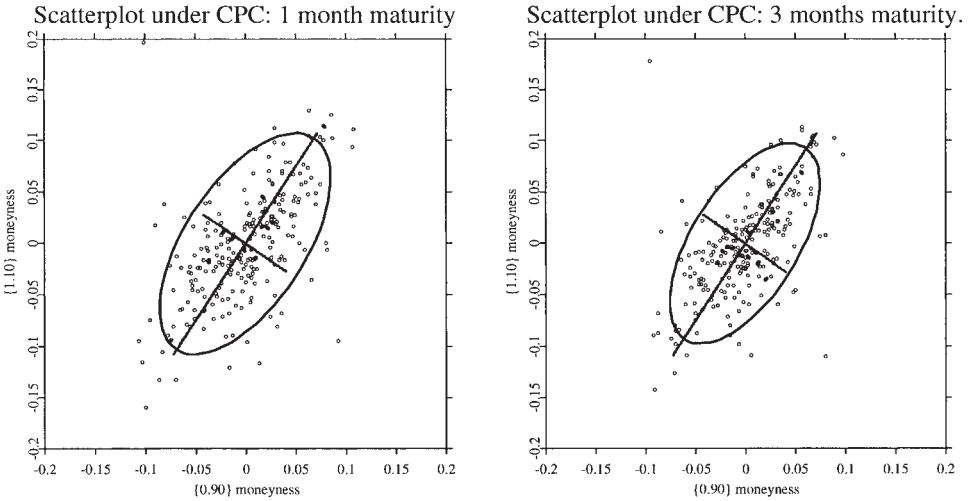

Figure 3. Scatterplots of implied volatility returns of moneyness $\kappa = 0.90$ against $\kappa = 1.10$ for groups of 1 month and 3 months time to maturity. Implied volatility computed as log-differences from the IVS recovered on a fixed grid; moneyness is defined as $K/(S_t e^{r\tau})$, where K is the strike and S_t the asset price (DAX value) in t, r the interest rate and $\tau = T - t$ time to maturity. The ellipse denotes the Mahalanobis distance defined in (1), which is the 95% confidence region for a bivariate normal distribution. Principle axes of the ellipses are the eigenvectors obtained by the CPC model for *both* maturity group, i.e., eigenvectors are estimated under the restriction to be identical, compare Figure 2.

model in which the eigenvectors are restricted to be common, i.e., their differences are attributed to sampling variability, while the eigenvalues (variances of the components) are allowed to be different. This is shown in Figure 3, which illustrates the same scatter plots with principal axes and ellipses estimated under the restriction of a common transformation of both groups, i.e., by assuming the model

$$\mathbf{\Psi}_1 = \mathbf{\Gamma}\mathbf{\Lambda}_1\mathbf{\Gamma}^\top \quad \text{and} \quad \mathbf{\Psi}_2 = \mathbf{\Gamma}\mathbf{\Lambda}_2\mathbf{\Gamma}^\top,$$

where $\mathbf{\Gamma}$ is an orthogonal transformation matrix and $\mathbf{\Lambda}_i = \text{diag}(\lambda_{i1}, \lambda_{i2})$ the matrices of eigenvalues in group $i = 1, 2$. Results are displayed in Table 2 for this CPC model. The formal presentation is delayed until Section 2.

For higher dimensional illustrations, consider the parallel coordinate plots in the three panels of Figure 4. Here, we display the six coordinates of the eigenvectors associated with the three largest eigenvalues. They are obtained by applying a PCA to each covariance matrix of IV returns separately in the maturity groups of one, two, and three months. Each group contains the full set of the moneyness grid, $\kappa \in \{0.85, 0.90, 0.95, 1.00, 1.05, 1.10\}$. Again, if the assumption of a common eigenstructure holds, we should expect the plots to deliver almost parallel lines. Clearly, this is the case.

The main advantages of the CPC approach compared to ordinary PCA lies in the fact that it is a way of compressing the high-dimensional (surface) data into a small number of factors that are common across groups. CPC models involve a smaller number of parameters to be estimated than ordinary PCA. Moreover, one avoids the consequences of pool-

Table 2. CPC in the Two Group Implied Volatility Case

Maturity Group	**1 Month**	**3 Months**
Estimated covariance	$\hat{\boldsymbol{\Psi}}_1 = \begin{pmatrix} 0.179 & 0.136 \\ 0.136 & 0.293 \end{pmatrix}$	$\hat{\boldsymbol{\Psi}}_2 = \begin{pmatrix} 0.144 & 0.110 \\ 0.110 & 0.235 \end{pmatrix}$
Matrix of eigenvectors	$\hat{\boldsymbol{\Gamma}}_{\text{CPC}} = \begin{pmatrix} 0.555 & 0.832 \\ 0.832 & -0.555 \end{pmatrix}$	
Characteristic roots	$\hat{\lambda}_1 = \begin{pmatrix} 0.383 & 0.089 \end{pmatrix}^\top$	$\hat{\lambda}_2 = \begin{pmatrix} 0.309 & 0.070 \end{pmatrix}^\top$

Notes: The table presents eigenvectors in the matrix $\hat{\boldsymbol{\Gamma}}_{\text{CPC}}$, eigenvalues $\hat{\lambda}_{ij}$ and estimated population covariance matrices $\hat{\boldsymbol{\Psi}}_i$ from a CPC analysis, the hypothesis of which is stated in (2). CPC analysis is applied to the groups of 1 and 3 months time to maturity implied volatility data: for each group $i = 1, 2$, sample covariance matrices (presented in Table 1) are computed from a two-dimensional time series of implied volatility returns calculated as log-differences. Each series belongs to a different moneyness in the IVS, 0.90 and 1.10, respectively. $\hat{\boldsymbol{\Psi}}_i$ and $\hat{\lambda}_{ij}$ are presented times 10^2. German DAX index option data.

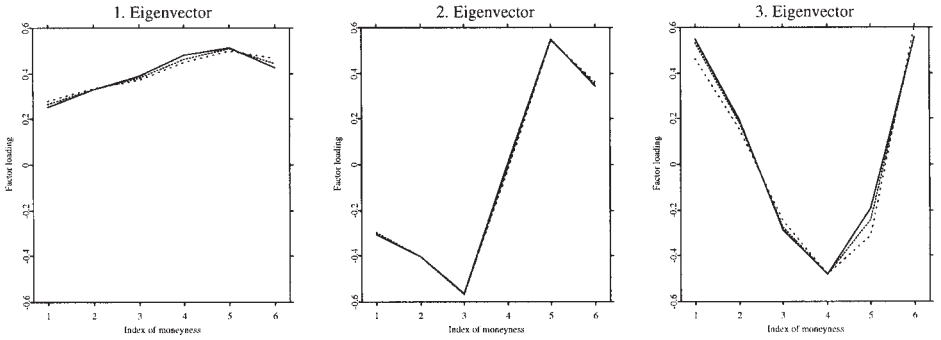

Figure 4. From left to right: first, second, and third eigenvectors obtained by a separate PCA for 1 month (solid), 2 months (dashed), 3 months (dotted) maturity group. Eigenvectors are shown as parallels coordinate plots. Index of moneyness 1–6 corresponds to moneyness $\kappa \in \{0.85, 0.90, 0.95, 1.00, 1.05, 1.10\}$, where moneyness is defined as $K/(S_t e^{r\tau})$. K is the strike and S_t the asset price (DAX value) in t, r the interest rate and $\tau = T - t$ time to maturity.

ing samples from different populations: hence the principal components are not distorted by between-group and within-group variability, and the group with highest variability does not largely determine the directions of the extracted components. In the context of the IVS analysis, this is an issue, since variability in front contracts is higher than for the longer maturities.

2. CPC models of the IVS

An inherent challenge of the analysis of IVs is the fact that for each observation date, the IVS is observed for different time to maturities, since options move towards their expiry dates. Thus, strictly speaking, differences or returns of IVs are not properly defined, and a smoothed or interpolated estimate of the IVS needs to be obtained. In the literature both parametric (Dumas, Fleming, and Whaley, 1998; Hafner and Wallmeier, 2001) and

nonparametric approaches are discussed (Aït-Sahalia and Lo, 2000; Cont and da Fonseca, 2002; Fengler and Wang, 2003). Since—given the discrete structure of the data—these global smoothing or fitting approaches may be considered as disadvantageous for certain applications, most recent approaches fit the surface nonparametrically only in the local neighborhood of the design points (Fengler, Härdle, and Mammen, 2003). However, since we are interested in the global forces driving the surface, we believe a daily fit of the surface to be a sufficiently good choice for our study. We use a nonparametric smoother, since it is difficult to justify a specific parametric form of the IVS.

The IVS is recovered on a grid of moneyness $\kappa_j \in \{0.85, 0.90, 0.95, 1.00, 1.05, 1.10\}$ and maturity $\tau_i \in \{1, 2, 3, 6, 9, 12\}$ months. In a second step we group the observations into maturity groups indexed by i and stack IV log-differences into multiple time series of the smile $\boldsymbol{X}_i$. Thus, we obtain $k = 6$ sample covariance matrices $\boldsymbol{S}_i$ of IV returns, which belong to different maturity groups i.

A first hypothesis concerning maturity groups in the IVS is the aforementioned CPC model. For covariance matrices $\boldsymbol{\Psi}_1, \ldots, \boldsymbol{\Psi}_k$ it is formally stated as

$$H_{\text{CPC}}: \quad \boldsymbol{\Psi}_i = \boldsymbol{\Gamma}\boldsymbol{\Lambda}_i\boldsymbol{\Gamma}^\top, \quad i = 1, \ldots, k. \tag{2}$$

$\boldsymbol{\Psi}_i$ are positive definite $p \times p$ population covariance matrices of IV returns, $\boldsymbol{\Gamma} = (\boldsymbol{\gamma}_1, \ldots, \boldsymbol{\gamma}_p)$ is an orthogonal $p \times p$ matrix of eigenvectors and $\boldsymbol{\Lambda}_i = \text{diag}(\lambda_{i1}, \ldots, \lambda_{ip})$ is the matrix of eigenvalues. The number of parameters to be estimated in the CPC model is $p(p-1)/2$ for the orthogonal matrix $\boldsymbol{\Gamma}$ plus kp for the eigenvalues in $\boldsymbol{\Lambda}_i$. The maximum likelihood estimates of $\boldsymbol{\Psi}_i$ are denoted by $\hat{\boldsymbol{\Psi}}_i = \hat{\boldsymbol{\Gamma}}\hat{\boldsymbol{\Lambda}}_i\hat{\boldsymbol{\Gamma}}^\top$, $i = 1, \ldots, k$. Sample common principal components of the maturity groups are given by $\boldsymbol{Y}_i = \hat{\boldsymbol{\Gamma}}^\top\boldsymbol{X}_i$.

A particular strength of CPC models is that they enclose a whole family of models with varying degrees of flexibility in the eigenstructure. The *proportional* model puts additional constraints on the matrix of eigenvalues $\boldsymbol{\Lambda}_i$ by imposing that $\lambda_{ij} = \rho_i\lambda_{1j}$, where $\rho_i > 0$ are unknown constants. This is equivalent to writing

$$H_{\text{prop}}: \quad \boldsymbol{\Psi}_i = \rho_i\boldsymbol{\Psi}_1, \quad i = 2, \ldots, k. \tag{3}$$

The number of parameters here is $p(p+1)/2 + (k-1)$. For the IVS this means that variances of the common components between the groups are proportionally scaled versions of each other. In terms of modelling the IVS, this implies that one needs to resort to one maturity group only, once the scaling constants ρ_i are estimated.

Leaving the assumptions on the eigenvalues as in hypothesis (2), one may ease the restrictions on the transformation matrix $\boldsymbol{\Gamma}$: this leads to *partial* CPC models, pCPC(q), where q denotes the order of common eigenvectors in $\boldsymbol{\Gamma}$. This is appropriate when one assumes that each maturity group is hit by q joint (big) shocks, and to a lesser extent by shocks differing among the different groups. This may be the case when heterogeneous trading takes place between long and short maturities distorting locally the surface. Formally, the hypothesis of the pCPC(q) model is

$$H_{\text{pCPC}}: \quad \boldsymbol{\Psi}_i = \boldsymbol{\Gamma}^{(i)}\boldsymbol{\Lambda}_i{\boldsymbol{\Gamma}^{(i)}}^\top, \quad i = 1, \ldots, k. \tag{4}$$

Table 3. Model Hierarchy of CPC Models[a]

Higher Model	Lower Model	Degrees of Freedom
Equality	Proportionality	$k-1$
Proportionality	CPC	$(p-1)(k-1)$
CPC[b]	pCPC(q) $(1 \leqslant q \leqslant p-2)$	$\frac{1}{2}(k-1)(p-q)(p-q-1)$
pCPC(1)	Arbitrary covariance matrices	$(p-1)(k-1)$

[a] The table presents the hierarchy of nested CPC models. From top to bottom restrictions on the estimated population covariance matrices are eased. Sequentially, starting from top, each CPC model is tested against the next lower one in the hierarchy. Degrees of freedom of the corresponding χ^2 test as given in column (3) are obtained by subtracting the number of parameters to be estimated in each model, compare (Flury, 1988, p. 151).

[b] First, CPC is tested against the pCPC($p-2$) model. Next, the pCPC($p-2$) model is tested against the pCPC($p-3$) model, etc., down to the pCPC(1) model.

where $\mathbf{\Lambda}_i$ is as in (2) and $\mathbf{\Gamma}^{(i)} = (\mathbf{\Gamma}_c, \mathbf{\Gamma}_s^{(i)})$. Here, the $p \times q$ matrix $\mathbf{\Gamma}_c$ contains the q common eigenvectors, while $\mathbf{\Gamma}_s^{(i)}$ of dimension $p \times (p-q)$ holds the $p-q$ group specific eigenvectors. The $\mathbf{\Gamma}^{(i)}$ are still orthogonal matrices. This implies that the necessary dimension p to estimate a pCPC(1) model is at least 3. When all possible pCPC(q) are to be estimated sequentially moving from the pCPC($p-2$) down to the pCPC(1) model, it is open to the modeling approach in which order the constraints on $\boldsymbol{\gamma}_j$ are relaxed. A natural way to proceed is to allow in each step for group specific eigenvectors in the 'least important' case, where 'least importance' is measured in terms of size of the corresponding eigenvalues. The total number of parameters amounts to $p(p-1)/2+kp+(k-1)(p-q)(p-q-1)/2$.

It is important to notice that the CPC and pCPC(q) models presented so far can be ordered in a hierarchical fashion, which allows a detailed analysis of the involved covariance matrices of different maturity groups. The highest level of similarity would be to assume equality between covariance matrices of different maturity groups $\mathbf{\Psi}_i$. In this case the number of parameters to be estimated is $p(p+1)/2$, and one may obtain the parameters by one single PCA applied to one pooled sample covariance matrix of all k groups. The models subsequently relaxing the restrictions are the proportional model and the CPC model. The following levels in the hierarchy are given by the pCPC(q) models starting from $q = p-2$ down to $q = 1$. The relations between different groups disappear subsequently, until at the last level the $\mathbf{\Psi}_i$ do not share any common eigenstructure. As all these different models are nested, one can decompose the total χ^2 statistic and test one model against a more flexible one in a 'step-up' procedure. Table 3 displays these sequential tests. By the summation property a test against any lower model is given by adding up the χ^2 test statistics and the degrees of freedom between the two models under comparison; additionally, we present Akaike and Schwarz information criteria.

3. Empirical Results

3.1. Presentation of the Data

Our data set contains daily data on DAX options from the German–Swiss Futures Exchange, EUREX for the entire year 1999 (254 trading days). Options are European style.

Table 4. Summary Statistics of Raw Implied Volatility Data

	Mean	Standard Deviation	Minimum	Maximum
Implied volatility	30.27%	8.41%	11.51%	79.97%
Moneyness	0.94	0.17	0.37	1.50
Time to maturity (years)	0.48	0.44	0.03	2.02

Notes: Summary statistics of the raw data used in this study. The implied volatility data is extracted from settlement option data on the German DAX index from 1999 (provided by EUREX). Implied volatilities are calculated by inverting the BS formula. Riskless interest rates are approximated by the EURIBOR (provided by Thomson Datastream) and interpolated linearly as to match the option's time to maturity. Moneyness is defined as $K/(S_t e^{r\tau})$, where K is the strike and S_t the asset price (i.e., DAX index value) in t, r the interest rate and $\tau = T - t$ time to maturity, measured in years.

Interest rate data and spot prices of the DAX are provided by Thomson Financial Datastream. For data preparation, the following procedure is applied to the 120401 observations of the initial database: first, we replace the prices of all in-the-money (ITM) options, whose prices possibly contain a liquidity premium, with the corresponding prices implied by the put-call parity. Specifically, we replace the price of each ITM call option by its out-of-the-money (OTM) put price. Thus all the information contained in liquid put prices is extracted and preserved in the corresponding call prices. Put prices may now be discarded without any loss of reliable information. Second, we omit options quoted less than one tick (€1/10), those with an IV greater than 80% (extreme far OTM options) and those with a time to maturity of less than 10 days because of their sensitivity to small errors. This filtering method leaves us with a final sample of 57702 observations, i.e., around 230 per day.

Table 4 describes the main features of the data set. Since the options are of European style, we, calculate the moneyness metric as the strike price K divided by the fair futures price F, i.e., K/F_t. We use the daily closing notation of the DAX from the German Stock Exchange and the term structure of the EURIBOR interest rate on a daily basis. The riskless interest rate of a given maturity is computed by linear interpolation. Finally, we calculate IVs. The smoothing method detailed in the Appendix is applied to obtain for each day the surface values of IVs on a given grid on moneyness and maturity. For the moneyness κ, we choose a grid off $\{0.85, 0.90, 0.95, 1.00, 1.05, 1.10\}$ and for maturity τ a grid of $\{1, 2, 3, 6, 9, 12\}$ months. This choice is led by availability of data (moneyess) and is to mimic the typical life time of option contracts. Thus we obtain 36 time series of the IVS, or from the perspective of the CPC model, six multivariate time series of the smile for a given maturity.

Summary statistics of the log-differences used for estimation are given in Table 5. There does not seem to be a large deviation from normality: skewness is positive-for the short and negative for the long maturities, however quite close to zero, and kurtosis is close to 3. We also perform Bera–Jarque-Tests on each single time series to test for normality in the data (Bera and Jarque, 1982). In only six out of 36 cases the hypothesis of normality is rejected at the 10% level of significance. More close inspection reveals that this finding is due to a singular distortion of the IVS at one particular date. Leaving this point out of the analysis, one cannot reject the hypothesis of normality. We take this as a justification of

Table 5. Summary Statistics of Implied Volatility Returns

Maturity Group	Mean	Stand. Dev.	Skewness	Kurtosis	Minimum	Maximum
1	−0.00032	0.051	0.026	3.259	−0.212	0.273
2	−0.00040	0.047	0.024	3.232	−0.212	0.261
3	−0.00052	0.044	0.010	3.248	−0.207	0.242
6	−0.00070	0.038	−0.002	3.167	−0.176	0.197
9	−0.00082	0.034	−0.027	3.175	−0.160	0.168
12	−0.00100	0.029	−0.046	3.228	−0.138	0.128

Notes: The table presents summary statistics of implied volatility returns computed as log-differences from the data described in Table 4. Before computing returns, daily implied volatility data is recovered on a regular grid by smoothing with a Nadaraya–Watson estimator, see Appendix A for details. Mean, standard deviation, skewness, and kurtosis are averaged across moneyness except for minimum and maximum. Time maturity is measured in months.

Table 6. Tests for Serial Correlation

Maturity Group	Lag	Moneyness					
	l	0.85			1.15		
		ρ_l	Q_l	p-value	ρ_l	Q_l	p-value
1	1	−0.183	8.432	0.004	−0.125	3.947	0.047
	2	−0.059	9.312	0.010	0.007	3.960	0.138
	3	−0.052	10.000	0.019	−0.091	6.032	0.110
	4	0.005	10.006	0.040	−0.084	7.809	0.099
12	1	−0.048	0.582	0.446	−0.119	3.590	0.058
	2	0.020	0.688	0.709	0.062	4.570	0.102
	3	−0.018	0.766	0.858	−0.029	4.788	0.188
	4	−0.057	1.595	0.810	−0.080	6.407	0.171

Notes: The table presents Box–Pierce-Statistics (Box and Pierce, 1970) Q_l for lags $l = 1, \ldots, 4$ to test for serial correlation in implied volatility returns. ρ_l denotes autocorrelation at lag l. Data is taken for moneyness 0.85 and 1.15 in the 1 and 12 months maturity group. For the definitions of moneyness see Table 4. p-values are obtained from a χ^2 distribution with l degrees of freedom.

our maximum likelihood approach assuming normality.

Some serial autocorrelation seems to be present especially in the short run IV returns, to a lesser extent in the groups with higher time to maturity. In Table 6, we report Box and Pierce (1970) statistics up to lag four for the opposite positions in the IVS, i.e., for moneyness 0.85 and 1.15 and for the 1 month maturity and 12 months maturity group. This is to present the 'extreme' cases. Due to these mixed results on autocorrelation we decided not to adjust the data. We believe the results not to be strongly affected by this simplification.

3.2. CPC Estimation Results

Consider first the data already presented in the separate PCA in Section 1. Covariance matrices are computed from log-differences of the multivariate time series of IVs. Tables 7–9

Table 7. Sample and Estimated Population Covariance Matrix of 1 Month Implied Volatility Returns

$$\boldsymbol{S}_1 = \begin{pmatrix} 0.1402 & 0.1460 & 0.1505 & 0.1217 & 0.1002 & 0.1221 \\ & 0.1822 & 0.2145 & 0.1784 & 0.1347 & 0.1366 \\ & & 0.2863 & 0.2360 & 0.1532 & 0.1328 \\ & & & 0.3000 & 0.3033 & 0.2208 \\ & & & & 0.4086 & 0.3023 \\ & & & & & 0.2898 \end{pmatrix}$$

$$\hat{\boldsymbol{\Psi}}_1 = \begin{pmatrix} 0.1505 & 0.1539 & 0.1554 & 0.1276 & 0.1096 & 0.1408 \\ & 0.1851 & 0.2121 & 0.175 & 0.1351 & 0.1485 \\ & & 0.2756 & 0.2218 & 0.1434 & 0.1363 \\ & & & 0.2754 & 0.2839 & 0.2205 \\ & & & & 0.3996 & 0.3127 \\ & & & & & 0.3211 \end{pmatrix}$$

Notes: This table presents the sample and estimated population covariance matrix of 1 month implied volatility returns (both times 10^2). Sample covariance matrix is computed from log-differences of implied volatilities recovered from a fixed grid of moneyness. The population covariance is estimated by $\hat{\boldsymbol{\Psi}}_1 = \hat{\boldsymbol{\Gamma}}\hat{\boldsymbol{\Lambda}}_1\hat{\boldsymbol{\Gamma}}^\top$, where $\hat{\boldsymbol{\Gamma}}$ denotes the matrix common eigenvectors and $\hat{\boldsymbol{\Lambda}}_1$ contains eigenvalues specific to group 1.

Table 8. Sample and Estimated Population Covariance Matrix of 2 Month Implied Volatility Returns

$$\boldsymbol{S}_2 = \begin{pmatrix} 0.1183 & 0.1305 & 0.1428 & 0.1194 & 0.0959 & 0.1093 \\ & 0.1621 & 0.1919 & 0.1588 & 0.1183 & 0.1230 \\ & & 0.2465 & 0.1954 & 0.1247 & 0.1212 \\ & & & 0.2411 & 0.2531 & 0.2038 \\ & & & & 0.3581 & 0.2813 \\ & & & & & 0.2642 \end{pmatrix}$$

$$\hat{\boldsymbol{\Psi}}_2 = \begin{pmatrix} 0.1228 & 0.1340 & 0.1450 & 0.1213 & 0.0987 & 0.1149 \\ & 0.1638 & 0.1916 & 0.1578 & 0.1183 & 0.1267 \\ & & 0.2434 & 0.1916 & 0.1217 & 0.1227 \\ & & & 0.2346 & 0.2468 & 0.2041 \\ & & & & 0.3530 & 0.2841 \\ & & & & & 0.2729 \end{pmatrix}$$

Notes: This table presents the sample and estimated population covariance matrix of 2 month implied volatility returns (both times 10^2). Sample covariance matrix is computed from log-differences of implied volatilities recovered from a fixed grid of moneyness. The population covariance is estimated by $\hat{\boldsymbol{\Psi}}_2 = \hat{\boldsymbol{\Gamma}}\hat{\boldsymbol{\Lambda}}_2\hat{\boldsymbol{\Gamma}}^\top$, where $\hat{\boldsymbol{\Gamma}}$ denotes the matrix common eigenvectors and $\hat{\boldsymbol{\Lambda}}_2$ contains eigenvalues specific to group 2.

display the three sample and the three estimated population covariance matrices. In Table 10 we present the model selection procedure. The step-up approach suggests a model, when the higher model is not rejected against the lower one, which is a pCPC(4) model here. The AIC is lowest for this model, but also very close to the AIC of the CPC model, while the SIC indicates exactly the CPC model. A test of the CPC model against the unrelated model yields 31.8, which corresponds to a p-value of 0.38 of the χ^2 distribution with 30 degrees of freedom.

Table 9. Sample and Estimated Population Covariance Matrix of 3 Month Implied Volatility Returns

$$S_3 = \begin{pmatrix} 0.1010 & 0.1162 & 0.1321 & 0.1123 & 0.0886 & 0.0974 \\ & 0.1415 & 0.1667 & 0.1367 & 0.1007 & 0.1092 \\ & & 0.2050 & 0.1572 & 0.0985 & 0.1086 \\ & & & 0.1879 & 0.2033 & 0.1825 \\ & & & & 0.3018 & 0.2540 \\ & & & & & 0.2376 \end{pmatrix}$$

$$\hat{\Psi}_3 = \begin{pmatrix} 0.0981 & 0.1139 & 0.1306 & 0.1107 & 0.0863 & 0.0920 \\ & 0.1411 & 0.1679 & 0.1382 & 0.1010 & 0.1058 \\ & & 0.2094 & 0.1617 & 0.1012 & 0.1072 \\ & & & 0.1955 & 0.2095 & 0.1825 \\ & & & & 0.3038 & 0.2503 \\ & & & & & 0.2269 \end{pmatrix}$$

Notes: This table presents the sample and estimated population covariance matrix of 3 month implied volatility returns (both times 10^2). Sample covariance matrix is computed from log-differences of implied volatilities recovered from a fixed grid of moneyness. The population covariance is estimated by $\hat{\Psi}_3 = \hat{\Gamma}\hat{\Lambda}_3\hat{\Gamma}^\top$, where $\hat{\Gamma}$ denotes the matrix common eigenvectors and $\hat{\Lambda}_3$ contains eigenvalues specific to group 3.

Table 10. Model Selection for Short Maturities Model—1, 2, 3 Months

Model		χ^2	df	p-val	AIC	SIC
Higher	**Lower**					
Equality	Proport.	237.0	2	0.00	352.0	352.0
Proport	CPC	82.7	10	0.00	118.0	127.7
CPC	pCPC(4)	7.1	2	0.03	55.7	111.3*
pCPC(4)	pCPC(3)	0.2	4	1.00*	52.6*	117.4
pCPC(3)	pCPC(2)	8.1	6	0.23	60.4	143.8
pCPC(2)	pCPC(1)	4.5	8	0.81	64.4	175.2
pCPC(1)	Unrelated	11.9	10	0.29	75.9	223.4
Unrelated					84.0	278.5

Notes: This table displays alternative model selection procedures for CPC models in the case of 1, 2, and 3 months maturity groups. Each line corresponds to a test of the higher model against the next lower one, compare also Table 3. From left to right, we present the two models to be compared, the value of the χ^2 test statistic, degrees of freedom (df), and the p-value (set-up procedure). Akaike (AIC) and Schwarz (SIC) information criteria are computed for the higher model given in column (1), see Appendix B.2 for definitions and details. Due to the nested nature of CPC models, tests spanning more than one step in the hierarchy can be directly read off from this table by adding the degrees of freedom and the values of the χ^2 test statistic. The asterisk * indicates the model preferred.

To sum up, each selection criterion advises us to accept a model which imposes a *common* eigenstructure on IV dynamics. The criteria only vary in the degree of additional constraints which one can assume, ranging from a CPC to pCPC(4) model. This ambiguity is not of importance from a modelling perspective of the IVS, as we will be interested in the first two or three components only: the first three components are common—be it a CPC or a pCPC(4) model.

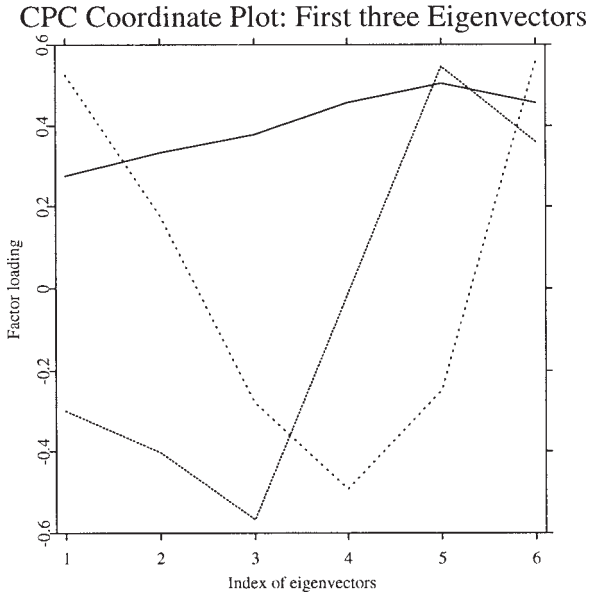

Figure 5. First (solid), second (dashed), and third (dotted) eigenvector obtained by the CPC model across the 1 month, 2 months, 3 months maturity group. Eigenvectors are shown as parallel coordinate plots. Index of moneyness 1–6 corresponds to moneyness $\kappa \in \{0.85, 0.90, 0.95, 1.00, 1.05, 1.10\}$, where moneyness is defined as $K/(S_t e^{r\tau})$. K is the strike and S_t the asset price (DAX value) in t, r the interest rate and $\tau = T - t$ time to maturity.

In Figure 5 we present the parallel coordinate plot for the three eigenvectors associated with the three biggest characteristic roots under CPC, see also Table 11. They have an intuitive interpretation: the first component has factor loadings that are all of the same sign. Thus, it can be interpreted as a 'shift shock'. The second eigenvector exhibits a Z-shaped structure: factor loadings have opposite sign at each side of the smile, which implies a differential impact on OTM puts and OTM calls. These second shocks are 'slope shocks'. The third characteristic vector displays a 'twist formation', giving a large weight to ATM IV returns and large weights of opposite sign to the outer parts of the smile: the curvature of the IVS is altered. These observations are in line with Skiadopoulos, Hodges, and Clewlow (1999), Fengler, Härdle, and Schmidt (2002) and Fengler, Härdle, and Mammen (2003).

The eigenvalues differ in size dropping from the shortest time to maturity to the biggest one. To evaluate the percentage of variance explained up to the mth component in the ith group we compute the quantity $\sum_{j=1}^{m} \lambda_{ij} / \sum_{j=1}^{p} \lambda_{ij}$. Altogether, the first three eigenvalues, $m = 3$, explain 98.5%, 98.9%, and 99.2% (one, two, and three months maturity) of the IVS variation. The relative proportion explained increases slightly, the longer the maturity, as can be seen in the right panel of Figure 6: whereas the first principal component explains 74.5% of all variability of the one month maturity, 77.5% are explained in the three months maturity group. This holds for the first two eigenvalues in all groups. Thus, while

Table 11. Estimation Results of the CPC Short Maturities Model—1, 2, 3 Months

$$\hat{\mathbf{\Gamma}}_{\text{CPC}} = \begin{pmatrix} 0.275 & -0.299 & 0.525 & -0.601 & 0.318 & 0.31 \\ (0.0085) & (0.0119) & (0.0153) & (0.0149) & (0.0174) & (0.0114) \\ 0.334 & -0.402 & 0.176 & -0.091 & -0.451 & -0.696 \\ (0.0099) & (0.0089) & (0.0091) & (0.0139) & (0.0201) & (0.013) \\ 0.379 & -0.567 & -0.278 & 0.374 & -0.207 & 0.524 \\ (0.014) & (0.0107) & (0.0134) & (0.0108) & (0.0177) & (0.0073) \\ 0.457 & -0.014 & -0.493 & -0.03 & 0.665 & -0.324 \\ (0.0038) & (0.0139) & (0.0072) & (0.0197) & (0.0104) & (0.0192) \\ 0.504 & 0.546 & -0.250 & -0.390 & -0.440 & 0.199 \\ (0.0135) & (0.0133) & (0.0139) & (0.0129) & (0.0112) & (0.0133) \\ 0.455 & 0.359 & 0.557 & 0.581 & 0.13 & -0.008 \\ (0.0099) & (0.015) & (0.0151) & (0.0137) & (0.0146) & (0.0077) \end{pmatrix}$$

$$\hat{\lambda}_1 = \begin{pmatrix} 1.197 & 0.289 & 0.097 & 0.018 & 0.004 & 0.001 \\ (0.1064) & (0.0257) & (0.0086) & (0.0016) & (0.0004) & (0.0001) \end{pmatrix}^\top$$

$$\hat{\lambda}_2 = \begin{pmatrix} 1.057 & 0.266 & 0.052 & 0.012 & 0.003 & 0.001 \\ (0.0940) & (0.0236) & (0.0046) & (0.0011) & (0.0004) & (0.0001) \end{pmatrix}^\top$$

$$\hat{\lambda}_3 = \begin{pmatrix} 0.910 & 0.236 & 0.020 & 0.007 & 0.002 & 0.001 \\ (0.0809) & (0.0210) & (0.0018) & (0.0006) & (0.0001) & (0.0001) \end{pmatrix}^\top$$

Notes: The table presents the estimation results of the CPC short maturities model, i.e., across the 1, 2 and 3 months maturity groups. Given are the estimated matrix of common eigenvectors $\hat{\mathbf{\Gamma}}_{\text{CPC}}$ and the group-specific eigenvalues $\hat{\lambda}_{ij}$, where $i = 1, 2, 3$. Eigenvalues are displayed as $\hat{\lambda}_{ij} \times 10^2$; standard errors in parenthesis.

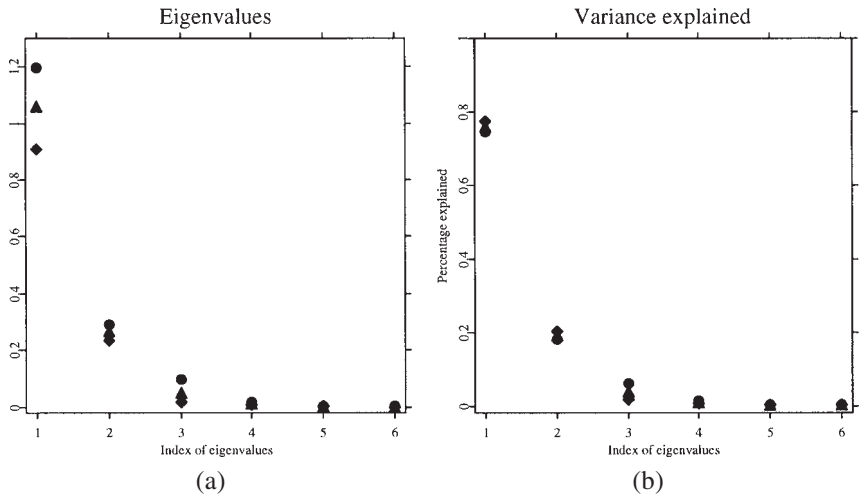

Figure 6. Eigenvalues (a) and the variance explained (b) as obtained in the CPC model: 1 month shown as circles, 2 months as triangles, 3 months as a rhombus. Variance explained of the mth component in group i is defined as $\hat{\lambda}_{im} / \sum_{j=1}^{p} \hat{\lambda}_{ij}$. Index 1–6 corresponds to moneyness $\kappa \in \{0.85, 0.90, 0.95, 1.00, 1.05, 1.10\}$.

Table 12. Model Selection for Long Maturities Model—6, 9, 12 Months

Model		χ^2	df	p-val	AIC	SIC
Higher	**Lower**					
Equality	Proport.	250.8	2	0.00	486.0	486.0
Proport	CPC	81.0	10	0.00	239.0	248.5
CPC	pCPC(4)	5.3	2	0.07	178.0	233.8
pCPC(4)	pCPC(3)	4.0	4	0.40	177.0	241.8
pCPC(3)	pCPC(2)	109.5	6	0.00	182.0	264.3
pCPC(2)	pCPC(1)	19.2	8	0.01	89.4	194.6*
pCPC(1)	Unrelated	16.2	10	0.09	83.6*	228.4
Unrelated					84.0	278.5

Notes: This table displays alternative model selection procedures for CPC models in the case of 6, 9, and 12 months maturity groups. Each line corresponds to a test of the higher model against the next lower one, compare also Table 3. From left to right, we present the two models to be compared, the value of the χ^2 test statistic, degrees of freedom (df), and the p-value (set-up procedure). Akaike (AIC) and Schwarz (SIC) information criteria are computed for the higher model given in column (1), see Appendix B.2 for definitions and details. Due to the nested nature of CPC models, tests spanning more than one step in the hierarchy can be directly read off from this table by adding the degrees of freedom and the values of the χ^2 test statistic. The asterisk * indicates the model preferred.

variability in principal components drops, the proportion of variance explained by the first principal components grows with increasing time to maturity. Beginning from the third eigenvalue this seems to be reversed. Consequently, the proportional model, which has more restrictive assumptions on the eigenvalues than the CPC model, cannot be appropriate for the IVS.

We also studied a full model by adding the six months and higher maturities to the short ones, but results are mixed. Therefore, we analyze the long maturities in a separate model with the covariance matrices of the six, nine and twelve months maturity only. Model selection is presented in Table 12. It deserves mentioning however that the factor loadings of the first two eigenvectors obtained from the short and the long time to maturity model are quite similar (up to sign).

The step-up approach suggests pCPC(4) or even CPC model at a 5% level, however, in direct tests against the unrelated model both are rejected. AIC is lowest for the pCPC(1). A test of the pCPC(1) against the unrelated model yields 16.2, which is χ^2-distributed with 10 degrees of freedom (p-value is 0.09). Hence one cannot reject pCPC(1) model for the long maturities. Indeed, at closer inspection of eigenvector obtained by a separate PCA, it is apparent that only the shift vector is similar. See Table 13 for the transformation matrix, where $\hat{\gamma}_1^c$ is the first common eigenvector, and $\hat{\gamma}_2^{(i)}$ and $\hat{\gamma}_3^{(i)}$ denote the specific ones. As can be seen, the latter differ. Possibly, the increased distance between maturities (three months as opposed to one month as before) 'loosens' the common structure observed in the short maturity groups. SIC favors the pCPC(2) model, and places pCPC(1) as second best.

For a better understanding on how the shocks are related to underlying asset price dynamics we compute the correlation with contemporaneous log-returns in the DAX index (here for the 3-maturity group, only): for the first component we find a correlation of -0.32. Thus level shocks are negatively correlated with the underlying, which can be inter-

Table 13. Estimation Results of the CPC Long Maturities Model—6, 9, 12 Months

Maturity Group i	1	2	3	1	2	3
$\hat{\mathbf{\Gamma}}^{(i)}_{\text{CPC}} =$	0.3127	0.3128	0.3150	0.3295	0.5379	0.4904	−0.1298
	0.3425	0.3980	0.4000	0.4056	0.1411	0.1300	−0.0873
	0.3783	0.5429	0.5395	0.5225	−0.3112	−0.2655	−0.0463
	0.4399	0.0079	0.0114	0.0214	−0.4812	−0.4855	0.5133
	0.4869	−0.5526	−0.5451	−0.5270	−0.2738	−0.3111	0.4111
	0.4594	−0.3787	−0.3901	−0.4190	0.5359	0.5826	−0.7354
$\hat{\lambda}_1 =$	0.675	0.177	0.024	0.005	0.001	0.0005
	(0.0401)	(0.0105)	(0.0014)	(0.0003)	(0.00006)	(0.00003)
$\hat{\lambda}_2 =$	0.548	0.148	0.011	0.003	0.001	0.0004
	(0.0326)	(0.0088)	(0.0007)	(0.0002)	(0.00004)	(0.00002)
$\hat{\lambda}_3 =$	0.389	0.113	0.004	0.001	0.001	0.0002
	(0.0231)	(0.0067)	(0.0003)	(0.0001)	(0.00003)	(0.00001)

Notes: The table presents the estimation results of the pCPC(1) long maturities model, i.e., across the 6, 9 and 12 months maturity groups. Given are the estimated single common and the first two group-specific eigenvectors of $\hat{\mathbf{\Gamma}}^{(i)}_{\text{CPC}} = (\boldsymbol{\gamma}^c_1, \boldsymbol{\gamma}^{(i)}_2, \boldsymbol{\gamma}^{(i)}_3)$, $i = 1, 2, 3$. The remaining three eigenvectors, the corresponding principal components of which account for less than 5% of the remaining variability, are omitted for sake of clarity. Group-specific eigenvalues $\hat{\lambda}_{ij}$ are provided. Eigenvalues are displayed as $\hat{\lambda}_{ij} \times 10^2$; standard errors in parenthesis.

preted as a 'leverage effect' (Black, 1976): according to this argument (implied) volatility rises, when there is a negative shock in the market value of the firms, since this results in an increase in the debt-equity ratio. For the second the third component correlation is close to zero (for the second component −0.09, for the third one 0.01).

To check for robustness, we divided the sample in three non-overlapping sub-samples of equal size and estimated the CPC models in each of them. Factor loadings changed only little, and model selection is found not to be altered in each sub-sample. Hence, we believe that the structure revealed remains reasonably stable during the sample period 1999.

Another form of robustness relates to bandwidth choice in the smoothing procedure and component extraction. Both are intricately linked, since different bandwidths result in different variance and bias of the estimates, but we are unaware of mathematical theory shedding light on this question. Even when smoothing and component estimation can be accomplished in one single step, this question seems to be mathematically unsolved (Kneip and Utikal, 2001). To assess robustness, we tried different bandwidths for smoothing. Clearly, the specific model selection is affected by changing bandwidths, but the overall picture of an eigenstructure of higher or lower degree of 'commonness' remains unaltered.

4. A CPC Factor Model for the IVS

Derman (1999) proposes models of the IV smile for a given maturity, which are known as 'sticky' rules. For any maturity, there is a linear relationship between the deviation of a fixed strike volatility from ATM volatility and the underlying price. The covariance structure as discovered in the CPC model leads to a standard factor model that generalizes

the Derman (1999) approach to the IVS and provides a dynamic version of the sticky models: for any maturity τ_i there will be a linear relationship between (log)-IVs and a small number of three *common* factors. The assumption of three factors is related to our decomposition of the IVS dynamics into three principal components identified as shift, slope and twist. In the following we formalize a factor model which allows for a scenario analysis in risk management or may serve as a partial model for a Monte Carlo pricing tool for exotic options.

As above, for any maturity τ_i denote $\sigma_t(\kappa_j, \tau_i)$ the IV at time t recovered on a given grid of moneyness κ_j, $j = 1, \ldots, p$. Smile dynamics of a fixed maturity τ_i can be modeled as

$$\Delta \ln \sigma_t(\tau_i) = \begin{pmatrix} \Delta \ln \sigma_t(\kappa_1, \tau_i) \\ \Delta \ln \sigma_t(\kappa_2, \tau_i) \\ \vdots \\ \Delta \ln \sigma_t(\kappa_p, \tau_i) \end{pmatrix} = \boldsymbol{B}(\tau_i)\boldsymbol{Y}_t(\tau_i) + \varepsilon_t(\tau_i) \tag{5}$$

$$= \sum_{j=1}^{m} \boldsymbol{b}_j(\tau_i)\boldsymbol{y}_{tj}(\tau_i) + \varepsilon_t(\tau_i), \tag{6}$$

where the unobservable variables $\boldsymbol{Y}_t(\tau_i)$ and $\varepsilon_t(\tau_i)$ are assumed to be i.i.d. distributed with

$$\mathsf{E}\big[\boldsymbol{Y}_t(\tau_i)\big] = 0, \qquad \mathsf{E}\big[\varepsilon_t(\tau_i)\big] = 0, \qquad \mathsf{Cov}\big[\boldsymbol{Y}_t(\tau_i), \varepsilon_t(\tau_i)\big] = 0.$$

This is, in fact, a maturity specific beta model: maturity specific dynamics in the smile, i.e., IV returns, are linearly linked to variables that are driving the movements of the IVS. The covariance structure identified in the CPC models can be exploited to characterize the model set-up more specifically. One identifies $\boldsymbol{b}_j(\tau_i) \stackrel{\text{def}}{=} \gamma_j$ and puts $\mathsf{Var}[\boldsymbol{y}_j(\tau_i)] = \lambda_{ij}$. If the model selection indicated a pCPC(q) model, then $\boldsymbol{b}_j(\tau_i) \stackrel{\text{def}}{=} \gamma_j^{(i)}$ beginning from $j \geqslant q$. Since the proceeding analysis revealed that the number of factors can be drastically reduced, we set $m = 3$.

The dimension reduction obtained is the corner stone of a model of the IVS dynamics: in a simple case, the proceeding model is specified for each maturity group i, while one group is chosen as reference group, e.g., the three-months maturity group. Shocks are generated by simulating from a normal distribution with variance $\mathrm{diag}(\lambda_{31}, \lambda_{32}, \lambda_{33})$, if $m = 3$. Shocks in other groups are interpreted as 'scaled' versions of the dynamics in group 3, and group-i-specific shocks are generated as simple multiples of the shocks in the reference group. Here, the entire surface dynamics are unfolded from $m = 3$ sources of shocks only.

In a more sophisticated set-up which allows for group specific shocks, one exploits the contemporaneous correlation structure across principal components in different maturity groups. Naturally, correlation is quite high with slightly decaying dependence between shocks the farer the groups are apart from each other. One generates random variables from an $(m \times k)$-dimensional normal distribution, where within-group correlation is zero and cross-group correlation as empirically found. Thus one allows for local distortions in the smile structure across the IVS, which is not possible in the first model outlined. In

this more sophisticated set-up, IVS dynamics are unfolded from mk shocks, k of which are highly correlated.

The procedure outlined above is useful for generating IVS scenarios for option portfolios. Worst case analysis or the computation of confidence regions for the scenarios can be based on Monte Carlo simulations (Jamshidian and Zhu, 1997; Fengler, Härdle, and Schmidt, 2002). Given the leverage interpretation of the first component, incorporating asset price dynamics to complete the model as a full pricing tool should be possible, but the in-depth analysis of the joint dependence is left for further research.

5. Conclusions

In this paper, we present a model that is capable of modeling the IVS dynamics, by reducing its dimension to a small number of factors *common* to several maturity groups. This is accomplished by working with a multivariate principal components technique that is designed for the multi-group case: *common* principal components. The common principal component analysis (CPC) exploits a group structure given by the data, and allows for jointly estimating a common eigenstructure across groups. This allows us to model the IVS returns simultaneously for different maturity groups. In a CPC framework several models with varying degrees of similarity in the eigenstructure can be compared and tested. The time series of IV returns we use are obtained by a nonparametric kernel smoothing procedure from German DAX option data from 1999.

The CPC model or a pCPC(4) model, where only four eigenvectors are shared across groups, is well justified for modeling the short maturities across the smile dynamics of IVs. In line with earlier literature, the shocks driving the IVS can largely be attributed to a shift, Z-shaped slope and twist shock. For the longer maturities a pCPC(1) can be a valid choice. The preferred modeling strategy is to assume that IVS dynamics obey a common eigenstructure or, equivalently, are driven by a small number of common factors.

The results have direct implications for the market models of volatility that aim at pricing illiquid or exotic options with observed IVs. By our evidence, the dimension of these models can be considerably reduced, because a common eigenstructure applies across different maturities. We demonstrate the power of CPC to reduce the dimension of IVS dynamics in presenting a factor model, which can be exploited in Monte Carlo based methods. Thus, identifying a common eigenstructure provides not only insights into low-dimensional dynamics driving high-dimensional objects, but also gives practical algorithms for risk management and IVS trading strategies.

Appendix A: IVS Smoothing and Bandwidth Choice

For a partition of explanatory variables $(x_1, x_2) = (\kappa, \tau)$, i.e., of moneyness and maturity, the two-dimensional Nadaraya–Watson kernel estimator of $\hat{\sigma}$ is given by

$$\hat{\sigma}(x_1, x_2) = \frac{\sum_{i=1}^{n} K_1((x_1 - x_{1i})/h_1) K_2((x_2 - x_{2i})/h_2) \hat{\sigma}_i}{\sum_{i=1}^{n} K_1((x_1 - x_{1i})/h_1) K_2((x_2 - x_{2i})/h_2)}, \tag{A.1}$$

where $\hat{\sigma}_i$ is the IV computed from observed option prices. $K_1(u)$ and $K_2(u)$ are univariate kernel functions, and h_1 and h_2 are the bandwidths. n denotes the number of observations. We use quartic kernels, i.e.,

$$K(u) = \frac{15}{16}\left(1 - u^2\right)^2 I\left\{|u| \leqslant 1\right\}, \tag{A.2}$$

where $I\{A\}$ is an indicator function assuming 1 when A is true, zero, otherwise. From an empirical point of view, the choice of the kernel function has little influence on the results.

As a selection procedure for the bandwidths h_1, h_2 we compute

$$n^{-1} \sum_{i=1}^{n} \left\{\hat{\sigma}_i - \hat{\sigma}_{h_1,h_2}(x_{1i}, x_{2i})\right\}^2 \times \Xi\left\{n^{-1} h_1^{-1} h_2^{-1} K_1(0) K_2(0)\right\}, \tag{A.3}$$

where $\Xi(u) \stackrel{\text{def}}{=} \exp(2u)$ is the Akaike penalizing function. Since alternative choices of penalizing functions have the same first order expansion, they asymptotically yield the same optimal smoothing parameters (Härdle, 1990). Next we average the penalized bandwidths across observation dates, which yields $h_1^* = 0.04$ in the moneyness and $h_2^* = 1.1$ in the maturity direction, at a standard deviation of $s(h_1) = 0.01$ and $s(h_2) = 0.12$, respectively. The low standard deviation of estimated bandwidths justifies using one single bandwidth for all estimation dates. However, bandwidths are still insufficient in both dimensions due to the discrete design of the data: data points appear like 'pearls in a necklace' in the three-dimensional space of the IVS. Penalizing approaches, as other cross validation procedures, evaluate the quality of the estimations right at actually observed data points. Since we need to obtain estimates at grid points deviating from the actual observations, bandwidths are too small. Hence in either dimension, oversmoothing with respect to the bandwidth as obtained from penalization precedure cannot be avoided. In finally using $h_1 = 0.1$, and $h_2 = 3.5$ for the surface up to the three months horizon, and $h_2 = 14.0$ for the long maturities, we also account for the fact that observations are closer in the front contracts than in the long term contracts (1 month distance compared to 3 months).

Appendix B: Estimating Common Eigenstructures

B.1. Maximum Likelihood Estimation

We only focus on the ordinary CPC model as formalized in (2), due to its similarity with the models (3) and (4) and its practical importance. For all other models as well as proofs and the asymptotic behavior of the estimates the reader is referred to Flury (1988).

Let $\boldsymbol{S}_i$ be the (unbiased) sample covariance matrix of implied volatilities, which are assumed to stem from an underlying p-variate normal distribution $\mathcal{N}_p(\mu, \boldsymbol{\Psi}_i)$. Sample size is $n_i > p$. The distribution of $\boldsymbol{S}_i$ is a generalization of the χ^2 variate, the Wishart distribution, with $n_i - 1$ degrees of freedom (Härdle and Simar, 2003):

$$n_i \boldsymbol{S}_i \sim \mathcal{W}_p(\boldsymbol{\Psi}_i, n_i - 1).$$

For the k Wishart matrices $\boldsymbol{S}_i$ the likelihood function is given by

$$L(\boldsymbol{\Psi}_1, \ldots, \boldsymbol{\Psi}_k) = c \prod_{i=1}^{k} \exp\left[\operatorname{tr}\left\{ -\frac{1}{2}(n_i - 1)\boldsymbol{\Psi}_i^{-1}\boldsymbol{S}_i \right\} \right] |\boldsymbol{\Psi}_i|^{-(1/2)(n_i-1)}, \tag{B.1}$$

where c is a constant not depending on the parameters. Maximizing the likelihood is equivalent to minimizing the function

$$g(\boldsymbol{\Psi}_1, \ldots, \boldsymbol{\Psi}_k) = \sum_{i=1}^{k} (n_i - 1)\left\{ \ln|\boldsymbol{\Psi}_i| + \operatorname{tr}\left(\boldsymbol{\Psi}_i^{-1}\boldsymbol{S}_i\right) \right\}. \tag{B.2}$$

Assuming that H_{CPC} in Equation (2) holds, yields

$$g(\boldsymbol{\Gamma}, \boldsymbol{\Lambda}_1, \ldots, \boldsymbol{\Lambda}_k) = \sum_{i=1}^{k} (n_i - 1) \sum_{j=1}^{p} \left(\ln \lambda_{ij} + \frac{\boldsymbol{\gamma}_j^{\top}\boldsymbol{S}_i\boldsymbol{\gamma}_j}{\lambda_{ij}} \right). \tag{B.3}$$

We impose the orthogonality constraints of $\boldsymbol{\Gamma}$ by introducing the Lagrange multiplyers μ_j for the p constraints $\boldsymbol{\gamma}_j^{\top}\boldsymbol{\gamma}_j = 1$, and the Lagrange multiplyer μ_{hj} for the $p(p-1)/2$ constraints $\boldsymbol{\gamma}_h^{\top}\boldsymbol{\gamma}_j = 0$, $(h \neq j)$. Hence the Lagrange function to be minimized is given by

$$g^*(\boldsymbol{\Gamma}, \boldsymbol{\Lambda}_1, \ldots, \boldsymbol{\Lambda}_k) = g(\cdot) - \sum_{j=1}^{p} \mu_j\left(\boldsymbol{\gamma}_j^{\top}\boldsymbol{\gamma}_j - 1\right) - 2\sum_{h<j}^{p} \mu_{hj}\boldsymbol{\gamma}_h^{\top}\boldsymbol{\gamma}_j. \tag{B.4}$$

Taking partial derivatives with respect to all λ_{ij} and $\boldsymbol{\gamma}_j$, it can be shown that the solution of the CPC model can be written as the generalized system of characteristic equations

$$\boldsymbol{\gamma}_m^{\top}\left\{ \sum_{i=1}^{k} (n_i - 1)\frac{\lambda_{im} - \lambda_{ij}}{\lambda_{im}\lambda_{ij}}\boldsymbol{S}_i \right\}\boldsymbol{\gamma}_j = 0, \quad m, j = 1, \ldots, p,\ m \neq j. \tag{B.5}$$

This is solved observing

$$\lambda_{im} = \boldsymbol{\gamma}_m^{\top}\boldsymbol{S}_i\boldsymbol{\gamma}_m, \quad i = 1, \ldots, k,\ m = 1, \ldots, p \tag{B.6}$$

and the constraints

$$\boldsymbol{\gamma}_m^{\top}\boldsymbol{\gamma}_j = \begin{cases} 0 & m \neq j, \\ 1 & m = j. \end{cases} \tag{B.7}$$

Flury (1988) proves existence and uniqueness of the maximum of the likelihood function, and Flury and Gautschi (1986) provide a numerical algorithm. All computations are made with Xplore (Härdle, Klinke, and Müller, 2000).

B.2. Testing and Model Selection

The log-likelihood ratio statistic for testing the H_{CPC} against the unrestricted model (unrelatedness between covariance matrices) is given by

$$T_{\text{CPC}} = -2 \ln \frac{L(\hat{\boldsymbol{\Psi}}_1, \ldots, \hat{\boldsymbol{\Psi}}_k)}{L(\boldsymbol{S}_1, \ldots, \boldsymbol{S}_k)} = \sum_{i=1}^{k} (n_i - 1) \ln \frac{|\hat{\boldsymbol{\Psi}}_i|}{|\boldsymbol{S}_i|}, \tag{B.8}$$

where $L(\boldsymbol{S}_1, \ldots, \boldsymbol{S}_k)$ denotes the unrestricted maximum of the log-likelihood. The statistic T_{CPC} is asymptotically χ^2 with $(k-1)p(p-1)/2$ degrees of freedom as $\min_{i=1}^{k} n_i \to \infty$ (Rao, 1973).

The CPC models presented are nested, since each model implies all models lower in the hierarchy. Thus one can decompose the total χ^2 into partial χ^2:

$$\begin{aligned} T_{\text{total}} = {} & T(\text{inequality of proportionality constants} \mid \text{proportionality}) \\ & + T(\text{deviation from proportionality} \mid \text{CPC}) \\ & + T\big(\text{nonequality of last } p-q \text{ components} \mid \text{pCPC}(q)\big) \\ & + T(\text{nonequality of the first } q \text{ components}). \end{aligned}$$

This decomposition of the log-likelihood is called step-up procedure (Flury, 1988).

Alternative model selection approaches are the AIC (Akaike, 1973) and SIC (Schwarz, 1978) criteria. The *AIC* is defined by

$$\begin{aligned} AIC = {} & -2 \times (\text{maximum of log-likelihood}) \\ & + 2 \times (\text{number of parameters estimated}). \end{aligned} \tag{B.9}$$

Following Flury (1988), we use a modified AIC. Assume we have U hierarchically ordered models to compare, with $r_1 < \cdots < r_u < \cdots < r_U$ parameters in model u. Define the *AIC* as:

$$AIC(u) = -2(L_u - L_U) + 2(r_u - r_1), \tag{B.10}$$

where L_u is the maximum of the log-likelihood function of model u. Selecting the model with the lowest *AIC* is equivalent to selecting the model with the lowest $AIC(u)$. Observe that $AIC(U) = 2(r_U - r_1)$ and $AIC(1) = -2(L_1 - L_U)$.

The *SIC*, which aims at finite dimensional models, is defined as

$$SIC = -2 \times (\text{maximum of log-likelihood}) \tag{B.11}$$

$$+ (\text{number of parameters estimated}) \times \ln(\text{number of observations}), \tag{B.12}$$

and is modified to

$$SIC(u) = -2(L_u - L_U) + (r_u - r_1) \ln(N), \tag{B.13}$$

where $N = \sum_{i=1}^{k} n_i$ denotes the overall sum of observations across the k groups. The model with lowest *SIC* is the best fitting one.

Acknowledgements

We gratefully acknowledge financial support from the Deutsche Forschungsgemeinschaft, Sonderforschungsbereich 373 "Quantifikation und Simulation ökonomischer Prozesse."

References

Aït-Sahalia, Y. and A. Lo. (2000). "Nonparametric Risk Management and Implied Risk-Aversion," *Journal of Econometrics* 94, 9–51.

Akaike, H. (1973). "Information Theory and an Extension of the Maximum Likelihood Principle." In *the 2nd International Symposium on Information Theory.* Budapest: Akademiai Kiado.

Alexander, C. (2001). "Principles of the Skew," *Risk* 14(1), S29–S32.

Avellaneda, M. and Y. Zhu. (1997). "An E-ARCH Model for the Term-Structure of Implied Volatility of FX Options," *Applied Mathematical Finance* 4, 81–100.

Basilevsky, A. (1994). *Statistical Factor Analysis and Related Methods: Theory and Applications*. Wiley Series in Probability and Mathematical Statistics. New York: Wiley.

Bates, D. (1996). "Jumps and Stochastic Volatility: Exchange Rate Processes Implicit in Deutsche Mark Options," *Review of Financial Studies* 9, 69–107.

Bera, A.K. and C.M. Jarque. (1982). "Model Specification Tests: A Simultaneous Approach," *Journal of Econometrics* 20, 59–82.

Black, F. (1976). "Studies of Stock Price Volatility Changes." In *Proceedings of the 1976 Meetings of the American Statistical Association*, pp. 177–181.

Black, F. and M. Scholes. (1973). "The Pricing of Options and Corporate Liabilities," *Journal of Political Economy* 81, 637–654.

Box, G.E.P. and D.A. Pierce. (1970). "Distribution of Residual Correlations in Autoregressive-Integrated Moving Average Time Series Models," *Journal of the American Statistical Association* 65, 1509–1526.

Cont, R. and J. da Fonseca. (2002). "The Dynamics of Implied Volatility Surfaces," *Quantitative Finance* 2(1), 45–602.

Derman, E. (1999). "Regimes of Volatility." In *Quantitative Strategies Research Notes*. Goldman Sachs.

Dumas, B., J. Fleming, and R.E. Whaley. (1998). Implied Volatility Functions: Empirical Tests," *Journal of Finance* 80(6), 2059–2106.

Derman, E. and M. Kamal. (1997). "The Patterns of Change in Implied Index Volatilities." In *Quantitative Strategies Research Notes*. Goldman Sachs.

Eberlein, E. and K. Prause. (2002). "The Generalized Hyperbolic Model: Financial Derivatives and Risk Measures." In H. Geman, D. Madan, S. Pliska, and T. Vorst (eds.), *Mathematical Finance—Bachelier Congress 2000.* New York: Springer, pp. 245–267.

Fengler, M.R., W. Härdle, and E. Mammen. (2003). "Implied Volatility String Dynamics," SfB 373 Discussion Paper, Humboldt-Universität zu Berlin.

Fengler, M.R., W. Härdle, and P. Schmidt. (2002). "Common Factors Governing VDAX Movements and the Maximum Loss," *Journal of Financial Markets and Portfolio Management* 16(1), 16–29.

Fengler, M.R. and Q. Wang. (2003). "Fitting the Smile Revisited: A Least Squares Kernel Estimator for the Implied Volatility Surface," SfB 373 Discussion Paper 2003-25, Humboldt-Universität zu Berlin.

Flury, B. (1988). *Common Principal Components and Related Multivariate Models.* Wiley Series in Probability and Mathematical Statistics. New York: Wiley.

Flury, B. and W. Gautschi.(1986). "An Algorithm for Simultaneous Orthogonal Transformations of Several Positive Definite Matrices to Nearly Diagonal Form," *Journal on Scientific and Statistical Computing* 7, 169–184.

Hafner, R. and M. Wallmeier. (2001). "The Dynamics of Dax Implied Volatilities," *International Quarterly Journal of Finance* 1(1), 1–27.

Härdle, W. (1990). *Applied Nonparametric Regression.* Cambridge, UK: Cambridge University Press.

Härdle, W., S. Klinke, and M. Müller. (2000). *Xplore—Learning Guide.* Heidelberg: Springer.

Härdle, W. and L. Simar. (2003). *Applied Multivariate Statistical Analysis*. Heidelberg: Springer.

Heston, S. and S. Nandi. (2000). "A Closed-Form GARCH Option Valuation Model," *Review of Financial Studies* 13, 585–625.

Hotelling, H. (1933). "Analysis of a Complex of Statistical Variables into Principal Components," *Journal of Educational Psychology* 24, 417–441.

Hull, J. (2002). *Options, Futures, and other Derivatives*. New York: Prentice Hall.

Hull, J. and A. White. (1987). "The Pricing of Options on Assets with Stochastic Volatilities," *Journal of Finance* 42, 281–300.

Jamshidian, F. and Y. Zhu, (1997). "Scenario Simulation: Theory and Methodology," *Finance and Stochastics* 1, 43–67.

Kneip, A. and K. Utikal. (2001). "Inference for Density Families Using Functional Principal Component Analysis," *Journal of the American Statistical Association* 96, 454, 519–531.

Ledoit, O. and P. Santa-Clara. (1998). "Relative Option Pricing with Stochastic Volatility," Working Paper, UCLA, Los Angeles, USA.

Mardia, K.V., J.T. Kent, and J.M. Bibby. (1992). *Multivariate Analysis,* 8th ed. New York: Academic Press.

Merton, R.C. (1973). "Option Pricing when Underlying Stock Returns Are Discontinuous," *Journal of Financial Economics* 3, 125–144.

Pearson, K. (1901). "On Lines and Planes of Closest Fit to Systems of Points in Space," *Philosophical Magazine* 2(6), 559–572.

Rao, C.R. (1973). *Linear Statistical Inference and Its Applications,* 2nd ed. New York: Wiley.

Rebonato, R. (1998). *Interest-Rate Option Models: Understanding, Analyzing and Using Models for Exotic Interest-Rate Options.* Wiley Series in Financial Engineering, 2nd ed. New York: Wiley.

Roll, R. (1977). "A Critique of the Asset Pricing Theory's Tests: Part I," *Journal of Financial Economics* 4, 129–176.

Schönbucher, P.J. (1999). "A Market Model for Stochastic Implied Volatility," *Philosophical Transactions of the Royal Society* 357, 1758, 2071–2092.

Schwarz, G. (1978). "Estimating the Dimension of a Model," *Annals of Statistics* 6, 461–464.

Skiadopoulos, G., S. Hodges, and L. Clewlow. (1999). "The Dynamics of the S&P 500 Implied Volatility Surface," *Review of Derivatives Research* 3, 263–282.

Stein, E.M. and J.C. Stein. (1991). "Stock Price Distributions with Stochastic Volatility: An Analytic Approach," *Review of Financial Studies* 4, 727–752.

Tompkins, R. (2001). "Stock Index Futures Markets: Stochastic Volatility Models and Smiles," *Journal of Futures Markets* 21(1), 43–78.